
ARTICLE

Development of a Realistic Computational Breast Phantom for Dosimetric Simulations

Andy K.W. MA* and Ali A. ALGHAMDI

Department of Radiological Sciences, University of Dammam, Dammam-31441, Saudi Arabia

Currently, x-ray breast imaging technique is the gold standard in both screening and diagnosis of breast cancer. However, x-rays, as a form of ionizing radiation, also post a risk of inducing cancer in the patients. As screening is applied to a large proportion of the population, the radiation dose from breast cancer screening is carefully monitored and it should necessarily be so. Since the breast cancer often grows in the glandular tissues of the breast, the mean glandular dose (MGD) is the commonly used quantity to indicate the radiation risk. In the estimation of the MGD, the breast tissues are actually assumed to be a homogeneous tissue in the Monte Carlo simulations of the energy deposition in the breast; together with the measurement of the entrance skin exposure, the simulated energy deposition provides the MGD estimate to a patient. In reality, the glandular tissue does not distribute in the breast uniformly; the accuracy of such estimates with homogeneous breast tissues has been questioned. To address the issue, we have developed realistic computational breast phantoms with anatomical details and mammographic texture. The anatomical details are composed of geometric objects while the mammographic texture is generated from the Fourier transform of Gaussian noise. Our new method will have implications in the reconstruction of the MGD for individual patients from their mammographic examinations. Our new phantoms will also have applications in dosimetric and imaging studies across x-ray based breast imaging modalities. Another application of the new phantom will be in the assessment and characterization of the 3D image reconstruction – The new phantom will allow us to quantify the reconstruction error. In this work, we will use the phantom to validate the conventional assumption of homogeneous breast tissue in the MGD calculations. The phantom generation software will be made available to the community through an open source arrangement.

KEYWORDS: *breast imaging, mean glandular dose, computational phantom*

I. Introduction

Breast cancer is the most common form of cancer in women. It is often treatable if detected early. Therefore, early detection is the aim of the breast cancer screening programs around the world. Currently, x-ray breast imaging technique is the gold standard in both screening and diagnosis of breast cancer. However, x-rays, as a form of ionizing radiation, also post a risk of inducing cancer in the patients. As screening is applied to a large proportion of the population, the radiation dose from breast cancer screening is carefully monitored and it should necessarily be so. Since the breast cancer often grows in the glandular tissues of the breast, the mean glandular dose (MGD) is the commonly used quantity to indicate the radiation risk. In the estimation of the MGD, the breast tissues are actually assumed to be a homogeneous tissue in the Monte Carlo simulations of the energy deposition in the breast; together with the measurement of the entrance skin exposure, the simulated energy deposition provides the MGD estimate to a patient.¹⁻⁴⁾ In reality, the glandular tissue does not distribute in the breast uniformly; the accuracy of such estimates with homogeneous breast tissues has been questioned.⁵⁾

The technology of breast imaging ranges from 2D film-based technology to advanced 3D methods such as

breast CT⁶⁾ and digital breast tomosynthesis.^{3,4,7)} Molecular imaging techniques such as positron emission mammography and breast specific molecular imaging are also under rapid development. All these new imaging modalities demand detailed imaging studies as well as dosimetric studies. The development of the DeBRa⁸⁾ breast phantoms fills in the gap between simple breast models for dosimetric studies and detailed models necessary in image formation simulations. It is because a DeBRa phantom has the anatomical structures and fine mammographic details to support both types of studies. It also has the potential in the study of imaging protocols for various modalities and image optimization without exposing the population with ionizing radiation.

The DeBRa phantom was primarily a tool for imaging studies. We have developed a software tool, Fatma, to construct realistic computational breast phantoms with anatomical details and mammographic texture for dosimetric studies. The Fatma programs were written in Scilab⁹⁾ which is an open-source platform for numerical computations. There are currently over 50 programs and graphical user interfaces (GUI) in the Fatma software tools to facilitate the creation and manipulation of the breast phantom. Thus, a breast phantom can be generated

- automatically by writing a Scilab main program that calls the modules in the Fatma tools; or
- interactively through the GUIs so that the user has

*Corresponding author, andyma@physics.org

control over most aspects of the phantom creation.

The Fatma tools include modules to export the phantom in XML format and MCNP(X) format. In this work, we used MCNPX 2.5.0¹⁰⁾ to estimate MGDs under simple irradiation conditions of monoenergetic x-ray beams. The results are compared with homogeneous breast phantoms of simple geometric shapes.

II. Materials and Method

1. Construction of the Breast Phantom

There are two aspects of a Fatma computational breast phantom – the anatomical features and the mammographic texture. The anatomical features include the external breast shape, the skin, the lactiferous ducts, the pectoral muscle and the Cooper’s ligaments. These features are constructed with combinatorial geometric solids of quadratic surfaces.^{8,11)} The external breast shape is described by the union of a partial one-sheet hyperbola and a semi-ellipsoid. The skin is modeled as a layer of uniform thickness between the external shape and the shape of the internal breast tissues underneath. The Cooper’s ligaments are ellipsoids and the lactiferous ducts are generated as a collection of cylinders in a bifurcation process starting from the nipple. The anatomical features are voxelized according to a user-specified dimension.

The compressed breast phantom was constructed by an arbitrary cropping of the external shape of a relaxed breast phantom; that is, the top and the bottom of the relaxed breast phantom were removed and only the central portion is retained. A layer of skin is made to cover the exposed internal volume after cropping. Then the internal anatomical details are generated as in the case of the relaxed breast phantom. Although this is not a real compression, it is suffice for the purpose of dosimetric simulations.

Figure 1(a) shows a rendering of a Fatma breast phantom in MLO view with a compressed breast thickness (CBT) of 4 cm, chest-wall-to-nipple distance (CND) 8 cm. The mammographic texture is generated from the Fourier transform of Gaussian noise.¹²⁾ It is then inserted into the voxelized phantom where there is no anatomical structure. The texture is interpreted as a collection of linear attenuation coefficients which give rise to different glandularities in the voxels. The texture is further modified by a sigmoidal function⁸⁾ to obtain the desired glandularity of the phantom. Glandularity is the mass fraction of fibroglandular tissues in the breast. The glandularity of the breast phantom is the average glandularity of the voxels. **Figure 1(b)** is a slice of the 3D texture matrix before insertion into the phantom and **Figure 1(c)** is a synthetic mammogram of the phantom generated by MCNPX radiography tally.

Further details of and the equations used in the construction of the phantom can be found in References 8, 11 and 12.

2. Construction of MCNPX Input Files

The MCNPX geometry is described by a combination of surfaces. An input file is composed of three sections for cell cards, surface cards and data cards respectively. Since the

Fatma phantom is a voxelized phantom, it is conveniently described by the lattice feature of the MCNPX code. Each lattice element corresponds to a voxel and each voxel is associated with a tissue type.

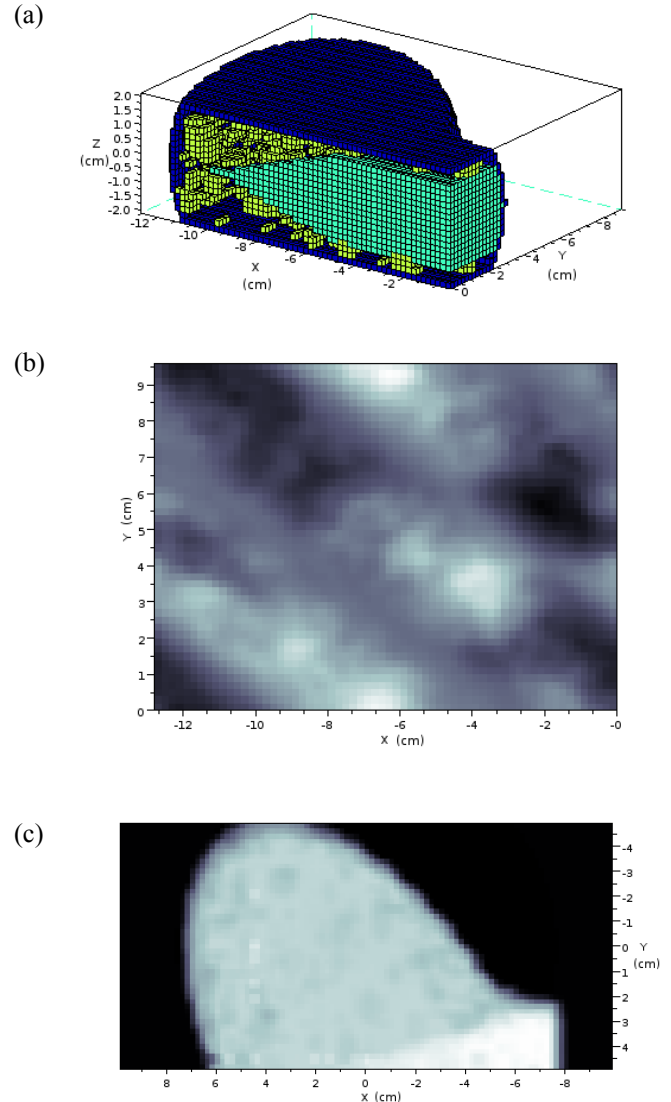


Fig. 1 Scilab rendering of a Fatma phantom (a) and its mammographic texture (b) whereas (c) is a “synthetic mammogram” generated by the MCNPX radiographic tally.

For MCNP(X) simulations, Fatma exports the phantom into four text files. The first one has “.cell” extension (Appendix A.1). It contains the description of how the surfaces are combined to construct the three-dimensional lattice and the list of the identity numbers of the tissue types. It also lists out the density of each tissue. The second file has “.surf” extension and it is the description of the surfaces (Appendix A.2). The third file contains the elemental compositions of the tissues and labeled with “.mtrl” extension (Appendix A.3). Elemental compositions and densities of the glandular and the adipose tissues come from literature.^{13,14)} The last file is the

tally description with “.tall” extension (Appendix A.4). Since Fatma is developed for MGD calculations, the “.tall” file contains the MCNPX DE/DF cards for modifying the energy deposition tallies. More specifically, the DE/DF cards from Fatma allow MCNPX to assign a portion, G , to the fibroglandular tissue in each voxel. G is a function energy and glandularity:³⁾

$$G = \frac{g \cdot (\mu_{en}/\rho)_{gland}}{g \cdot (\mu_{en}/\rho)_{gland} + (1-g) \cdot (\mu_{en}/\rho)_{adipose}}, \quad (1)$$

where g is the glandularity; $(\mu_{en}/\rho)_{gland}$ and $(\mu_{en}/\rho)_{adipose}$ are the mass energy absorption coefficients of the glandular and the adipose tissues respectively.

The main simulation input file (Appendix A.5) includes the geometry outside the breast phantom, the x-ray source definition and other data cards necessary for the simulation. In the example of Appendix A.5, the geometry is consisted only of a sphere of air outside the breast phantom. It reads in the “.cell” file in the cell card section, the “.surf” file in the surface card section and the “.mtrl” and the “.tall” files in the data card section. In this way, input files for simulations of the same breast under different conditions can easily be constructed and carried out. To obtain the simulated mammogram in Figure 1(c), the main input file in the appendix was modified such that a radiography tally replaced the f6 tally and the read file card for the “.tall” file was omitted.

3. Simulations

Several of simulations have been carried out for this work with one set being with the Fatma phantom of heterogeneous breast tissues and the other with simple geometric shapes of homogeneous breast tissues. In each simulation, the x-ray source was a cone beam of 15 keV monoenergetic photons located 48 cm above the top surface of the breast phantom.

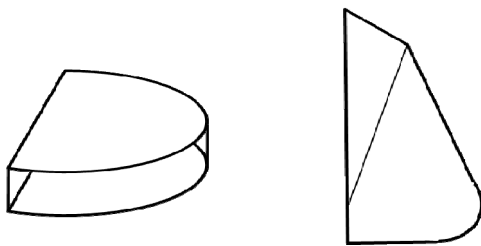


Fig. 2 The external shape of the simple CC (left) and MLO (right) phantoms for MGD calculations. The CC phantom does not have the pectoral muscle while the MLO phantom has. Please refer to the text for more details.

For the simulations of the homogeneous breast tissue approximation, a CC-view and an MLO-view phantom were constructed from simple geometric shapes (**Fig. 2**). The CC-view phantom is a semi-circular disc with radius 8 cm and thickness 4 cm. The breast tissue is assumed to be 50-50 homogeneous mixture of glandular and adipose tissues (0.5 glandularity) surrounded by 0.5-cm of adipose tissue sheath.²⁾

The MLO-view phantom is constructed according to Reference 3. Its glandularity is also 0.5 and surrounded by 0.5-cm adipose tissue sheath. These two phantoms are called unstructured phantoms because they do not have any anatomical structures while the Fatma phantom is a structured phantom.

III. Results and Conclusion

MGD calculations are usually normalized by the entrance skin kerma or entrance skin exposure. Both the entrance skin kerma and the entrance skin exposure are measured without backscattering from the breast. The unit for MGD is mGy/mGy. Since this work is comparing the MGD in simple irradiation geometry, the air kerma or exposure just before entering the breast phantom is the same for all simulations. Therefore we left the results in the unit of MeV/g per source photon. **Table 1** is the summary.

Table 1 Results of the simulations

	MeV/g/src	Relative error
Structured Fatma phantom	6.6×10^{-6}	2%
Unstructured MLO phantom	5.4×10^{-6}	1%
Unstructured CC phantom	5.5×10^{-6}	1%

In spite of the difference in the shapes of the unstructured MLO and CC phantoms, the calculated MGDs differ by less than 2%. This is similar to results of an x-ray beam directly above the phantoms in previous work by other authors^{3,4)}. On the other hand, The structured Fatma phantom has a shape similar to the unstructured MLO phantom but the MGD from the Fatma phantom is 22% higher than the MLO phantom. Thus the glandular structure in the breast tissue is an important factor in the estimation of the MGD.

This result here is also in line with the results of Reference 5 in which the authors found a 9% to 59% difference between the structured phantom and the unstructured phantom. However, the construction of the Fatma phantom is very different from that in Reference 5. Therefore, our results could be an independent verification of earlier attempts by other researchers.

It is clear that this is a preliminary study with a single phantom. Further work is necessary to ascertain if the same conclusion is valid under realistic irradiation conditions. Furthermore, it is important to demonstrate the same in the emerging breast imaging modalities such as digital breast tomosynthesis and breast CT. It has been shown that the MGD in digital breast tomosynthesis in MLO view has a strong dependence on the irradiation angle since the x-ray source moves along an arc over the breast.^{3,4)} The glandular structure might have stronger effects on the MGD under digital breast tomosynthesis.

From a 2D mammogram, be it a film/screen-based or from full-field digital mammography, we cannot derive the true 3-dimensional distribution of the fibroglandular tissue with confidence. Thus, we cannot translate the results from the structured breast phantoms to a clinically relevant MGD calculation and it is not recommended to change the current

practice of MGD estimation.⁵⁾ On the other hand, there is a trend towards the 3D modalities such as tomosynthesis and breast CT. Such modalities can provide a good approximate distribution of the fibroglandular tissues. Then, a Monte Carlo based calculation from a structured phantom may give rise to a revision in the MGD estimation. It may lead to a personalized MGD estimation as well.

In this paper, we have also presented the software tool Fatma for constructing realistic breast phantoms for dosimetric studies. Although Fatma was developed for dosimetric studies, it is conceivable to incorporate new modules in the software collection so that tumors and microcalcifications are available for imaging simulations.⁸⁾ Another line of development is to introduce a compression module so that a CC-view or an MLO-view phantom is obtained from the compression of a relaxed breast phantom. This module will add further realism in the model and will open up new applications of the Fatma breast phantom. It can be obtained by sending an email to fatma.phantom@gmail.com with “request phantom” in the subject line.

References

- 1) J. M. Boone, “Glandular breast dose for monoenergetic and high-energy x-ray beams: Monte Carlo assessment,” *Radiology*, **213**, 23–37 (1999).
- 2) D. R. Dance, “Monte Carlo calculation of conversion factors for the estimation of mean glandular breast dose,” *Phys. Med. Biol.*, **9**, 1211–1219 (1990).
- 3) A.K.W. Ma, D.G. Darambara, A. Stewart, S. Gunn, E. Bullard, “Mean glandular dose estimation using MCNPX for a digital breast tomosynthesis system with tungsten/aluminum and tungsten/aluminum+silver x-ray anode-filter combinations,” *Med. Phys.*, **35**, 5278–5289 (2008).
- 4) I. Sechopoulos, S. Suryanarayanan, S. Vedantham, C. D’Orsi, A. Karellas, “Computation of the glandular radiation dose in digital tomosynthesis of the breast,” *Med. Phys.*, **34**, 221–232 (2007).
- 5) D. R. Dance, R. A. Hunt, P. R. Bakic, A. D. A. Maidment, M. Sandborg, G. Ullman, G. A. Carlsson, “Breast dosimetry using high-resolution voxel phantoms,” *Radiat. Prot. Dosim.*, **114**, 359–63 (2005).
- 6) J. M. Boone, T. R. Nelson, K. K. Lindfors, J. A. Seibert, “Dedicated breast CT: Radiation dose and image quality evaluation,” *Radiology*, **221**, 657–667 (2001).
- 7) L. T. Niklason, B. T. Christian, L. E. Niklason *et al.*, “Digital tomosynthesis in breast imaging,” *Radiology*, **205**, 399–406 (1997).
- 8) A. K. W. Ma, S. Gunn, D. G. Darambara, “Introducing DeBRa: A detailed breast model for radiological studies,” *Phys. Med. Biol.*, **54**, 4533–4545 (2009).
- 9) www.scilab.org
- 10) D. B. Pelowitz (ed.), *MCNPX™ User’s Manual*, LA-CP-05-0369, Los Alamos National Laboratory (2005).
- 11) K. Bliznakova, Z. Bliznakov, V. Bravou, Z. Kolitsi1, N. Pallikarakis, “A three-dimensional breast software phantom for mammography simulation,” *Phys. Med. Biol.*, **48**, 3699–3719 (2003).
- 12) J. M. Shorey, *Stochastic simulations for the detection of objects in three dimensional volumes: applications in medical imaging and ocean acoustics*, PhD Thesis, Duke University (2007).
- 13) G. R. Hammerstein, D. W. Miller, D. R. White, M. E. Masterson, H. Q. Woodard, J. S. Laughlin, “Absorbed radiation dose in mammography,” *Radiology*, **130**, 485–91 (1979).
- 14) www.nist.gov/physlab/data/index.cfm

Appendix

A.1. The .cell file

This file (**Fig. A1**) describes the geometry of the voxels in the phantom. Cell 901 defines the three-dimensional extent of the phantom while cell 900 defines that of the voxel at the centre of the phantom, through combinations of surfaces. The surfaces are labeled 911, 912 and so on. The parameters of these surfaces are defined in the .surf file (Appendix A.2). The “+” and “-” signs give which side of the surface should be considered to form the three-dimensional cell. “trcl=901” in the cell definition instructs MCNPX to apply a transformation on the phantom such that the phantom is constructed at origin but simulated at a different location. The transformation is specified in the main input file (Appendix A.5).

Furthermore, the “fill=900” instruction tells MCNPX to fill the phantom (cell 901) with voxels (cell 900). The number of voxels in each dimension is specified by the “fill=-32:32 -24:24 -10:10” instruction. The content of each voxel, that is, the type of tissue or air, is specified by the long list of numbers starting with “255 8r 1 54r ...” until 1 5r 255 498r” with hundreds of lines omitted in this partial listing. Air must be included simply to fill up the voxels outside the breast phantom and that the attenuation of the mammographic x-rays is important in MGD calculations.

The letter “r” after a number in the tissue list represents the number of repetitions of the tissue. For examples, “255 8r” means that whatever tissue 255 is, the voxel is repeated 9 times; similarly, “1 54r” means that tissue 1 is repeated 55 times.

```

c
c Fatma breast phantom - CELL cards
c
900 0 -913 912 -923 922 -933 932
lat=1 fill = -32:32 -24:24 -10:10
255 8r 1 54r 255 9r 1 54r 255 8r 1 55r 255 8r 1 55r 255 7r 1
56r 255 7r 1 56r 255 7r 1 56r 255 6r 1 57r 255 6r 1 57r 255 6r 1 57r 255
6r 1 57r 255 5r 1 53r 255 10r 1 50r 255 13r 1 47r 255 16r 1 46r 255 17r 1
46r 255 17r 1 45r 255 17r 1 45r 255 18r 1 44r 255 19r 1 44r 255 19r 1
43r 255 20r 1 42r 255 21r 1 41r 255 22r 1 41r 255 22r 1 40r 255 23r 1
:
:
:
21r 1 41r 255 22r 1 41r 255 22r 1 40r 255 23r 1 39r 255 24r 1 38r 255
26r 1 36r 255 27r 1 35r 255 28r 1 34r 255 29r 1 33r 255 31r 1 31r 255
32r 1 30r 255 33r 1 28r 255 36r 1 26r 255 38r 1 24r 255 39r 1 22r 255
42r 1 19r 255 46r 1 15r 255 49r 1 12r 255 54r 1 5r 255 498r
u=900 imp:p=1
c
1 1 -1.090000e+00 -909 u= 1 imp:p=1 $skin
3 3 -1.050000e+00 -909 u= 3 imp:p=1 $skeletal muscle
100 100 -9.212000e-01 -909 u= 100 imp:p=1 $mammo100
101 101 -9.236000e-01 -909 u= 101 imp:p=1 $mammo101
102 102 -9.260000e-01 -909 u= 102 imp:p=1 $mammo102
:
:
:
146 146 -1.031600e+00 -909 u= 146 imp:p=1 $mammo146
147 147 -1.034000e+00 -909 u= 147 imp:p=1 $mammo147
148 148 -1.036400e+00 -909 u= 148 imp:p=1 $mammo148
149 149 -1.038800e+00 -909 u= 149 imp:p=1 $mammo149
255 255 -1.230000e-03 -909 u= 255 imp:p=1 $air
901 0 -914 911 -924 921 -934 931 fill=900 trcl=901 imp:p=1
c
c Fatma breast phantom - CELL cards End
c

```

Fig. A1 Partial listing of an example “za03.cell” file

The cells 1, 3, 100 and 101 to 149 are the tissues of the breast phantom; 255 is the air outside the phantom. The elemental compositions of the tissues and air are specified in the .mtrl file (Appendix A.3). However, the density of each material is specified here. For example, skin is tissue 1; its cell label is 1 (first one in the line) and its material label is also 1 (second one in the line); its density is 1.09 g/cm^3 . The “-“ sign in front of the value signifies the unit as g/cm^3 . As another example, skeletal muscle is tissue 3, cell label 3 and material label 3; its density is 1.05 g/cm^3 . Tissues corresponding to the mammographic texture are labeled from 100 to 149. Their elemental compositions and densities are derived from the assumed linear attenuation coefficients as described in the text. Further details of the MCNP input file format can be found in Reference 10.

A.2. The .surf file

This file (Fig. A2) describes the type and the parameters of the surface in the construction of the three-dimensional cells in the .cell file. Surface 909 is of type “so” which is a sphere at the origin and of radius 0.246211 cm corresponding to the longest diagonal of a voxel. Surfaces 911 to 934 are of types “px”, “py” and “pz” – planes perpendicular to one of the three axes x, y and z. The values specify where the planes are intersecting the axis in cm.

```

c
c Fatma breast phantom - SURFACE cards End
c
c 909 so 8.246211
c
c 911 px -6.399900
c 912 px 0.000000
c 913 px 0.200000
c 914 px 6.599900
c
c 921 py -4.799900
c 922 py 0.000000
c 923 py 0.200000
c 924 py 4.999900
c
c 931 pz -1.999900
c 932 pz 0.000000
c 933 pz 0.200000
c 934 pz 2.199900
c
c Fatma breast phantom - SURFACE cards End
c

```

Fig. A2 Full listing of an example “za03.surf” file

A.3. The .mtrl file

This file (Fig. A3) specifies the elemental composition of each tissue in the breast phantom. Each elemental is represented by a six-digit number such that the first three digits are the atomic number and the last three are the mass number. In photon and electron cross sections, the isotope is ignored and therefore the last three digits are always zero. For examples, 1000 is hydrogen and 11000 is sodium. The negative value is the mass fraction of the element in the tissue.

A.4. The .tall file

This file (Fig. A4) contains the dosimetric tallies for simulations. The values following the “vol” line are the volumes of the tissues in cm^3 . They are computed from the number of voxels of each tissue and their dimensions. The f6 tallies estimate the amount of energy deposition in the volume and by the particle specified in the tally. The result is norma-

```

c
c Fatma breast phantom - MATERIAL cards
c
c skin
m1 1000 -0.100588
6000 -0.228250
7000 -0.046420
8000 -0.619002
11000 -0.000070
12000 -0.000060
:
:
:
c mammo100
m100 1000 -0.119280
6000 -0.632123
7000 -0.008241
8000 -0.237353
11000 -0.000494
12000 -0.000020
15000 -0.000172
16000 -0.000736
17000 -0.001177
19000 -0.000330
20000 -0.000034
26000 -0.000020
30000 -0.000020
c
c mammo101
m101 1000 -0.118887
6000 -0.621929
7000 -0.008782
8000 -0.247354
11000 -0.000483
:
:
:
c
c air
m255 6000 -0.000124
7000 -0.755267
8000 -0.231781
18000 -0.012827
c
c
c Fatma breast phantom - MATERIAL cards End
c

```

Fig. A3 Partial listing of an example “za03.mtrl” file

```

c
c Fatma breast phantom - TALLY cards
c
c #
c vol
c j
45.752000 $tissueID 1
36.064000 $tissueID 4
24.936000 $tissueID 5
0.024000 $tissueID 100
0.056000 $tissueID 101
0.024000 $tissueID 102
:
:
:
204.832000 $tissueID 255
c
c mammo101
f16:p (101<900)
fc16 g, mg, & nVox = 0.022550, 0.000188, 7
c
de16 1.000e-03 1.500e-03 2.000e-03 3.000e-03 4.000e-03 5.000e-03 6.000e-03
8.000e-03 1.000e-02 1.500e-02 2.000e-02 3.000e-02 4.000e-02 5.000e-02
6.000e-02 8.000e-02 1.000e-01 1.500e-01 2.000e-01 3.000e-01 4.000e-01
5.000e-01 6.000e-01 8.000e-01 1.000e+00 1.250e+00 1.500e+00 2.000e+00
3.000e+00 4.000e+00 5.000e+00 6.000e+00 8.000e+00 1.000e+01 1.500e+01
2.000e+01
c
df16 2.870e-02 2.944e-02 2.991e-02 3.031e-02 3.083e-02 3.153e-02 3.178e-02
3.212e-02 3.236e-02 3.272e-02 3.278e-02 3.188e-02 2.960e-02 2.675e-02
2.434e-02 2.166e-02 2.062e-02 1.992e-02 1.970e-02 1.972e-02 1.971e-02
1.970e-02 1.970e-02 1.970e-02 1.970e-02 1.970e-02 1.970e-02 1.972e-02
1.970e-02 1.907e-02 1.996e-02 2.007e-02 2.026e-02 2.043e-02 2.079e-02
2.105e-02
c
:
:
:
c
c
c Fatma breast phantom - TALLY cards End
c

```

Fig. A4 Partial listing of an example “za03.tall” file

lized by the mass of the volume and by the number of source particles simulated. The unit is MeV/g per source particle. Each f6 tally is labeled by a number in a multiple of 10 plus 6. Thus f6, f16, f26 and so on are all energy deposition tallies of the same type. In Fig. A4, f16 estimates the dose to tissue 101 (represented by the string “101< 900”) by photons (the symbol “p” after f16).

The line fc16 is simply a line of comment in the simulation output file to aid tally identification. They are also supplying the necessary information to the post-simulation processing to estimate the MGD to the whole breast. The three values represent the glandularity (g) of the fibroglandular tissue, its mass in g (mg) and the number of such voxels in the breast phantom (nVox). The “de” and “df” cards together defines the tally modifying function. The de card defines the energy bins in MeV while the df card defines the G-values in Eq. (1). The number of f6 tallies depends on the number of different fibroglandular tissues.

A.5. The MCNPX Main Input File

This file (Fig. A5) is an example of the main input file to use the Fatma phantom. The first line in the file is the problem identification of the simulation. It is followed by three sections separated by two blank lines. The first section is the cell definitions. The main input file reads in the .cell file here. Also included in this section are the cell definitions for the geometry outside the phantom. The geometry may include the body of the patient and the mammography equipment. In this example, only a sphere enclosing the simulation is specified (cell 990). Beyond it is cell 991 where the particle will be terminated.

The second section is the surface definitions. The .surf file is read in here. As in the cell definition section, the surfaces of the geometry outside the phantom are specified. In this example, the sphere is 100 cm in radius located at the origin.

The last section is the data section that contains the material definitions, the tally specifications and other simulation parameters. Therefore, the .mtrl and the .tall files are read in here. Since air (material 255) is already specified in the .mtrl

```
Fatma main input file
c CELL CARDS
c read fatma cells
read file=za03.cell
c
c cells outside fatma
990 255 -1.23e-3 -990 #901 imp:p=1
991 0 +990 imp:p=0
c END CELL CARDS

c SURFACE CARDS
c read fatma surfaces
read file=za03.surf
c
c surfaces outside fatma
990 so 100
c END SURFACE CARDS

c DATA CARDS
c read fatma material
read file=za03.mtrl
c
c read fatma MGD tallies
read file=za03.tall
c
mode p
c
*tr901 0 0 0
c
sdef par=p erg=0.015 pos=0 0 50 vec=0 0 -1 dir=d2
si2 0.98 1.0
sp2 0.0 1.0
c
prdmp j -360 1
c
nps 1e7
c END DATA CARDS
```

Fig. A5 Listing of an example main MCNPX input file

file, the definition of air need not be repeated in the main input file. Should there be other materials required in the simulation geometry, there are to be defined here.

As mentioned in Appendix A.1, the phantom is construction at origin but it may be simulated at a location within the mammography machine. Transformation 901 must be defined here. This example input file does not move the phantom to a new location and therefore the “tr901” card has only three 0s representing no translation. If desired, the card allows translation and rotation of the phantom.

The “mode” card, the “sdef” card and the “nps” card instruct MCNPX to simulation a beam of 10 million source photons at 15 keV and covering the whole phantom. Interested readers may consult the MCNPX manual¹⁰⁾ for further information.